Supplementary information

Supplementary Materials and Methods

Reagents

Antibodies against cleaved caspase-3, β-tubulin, pAkt (S473), pGSK3β (S9), Akt, ErbB2, MEK, and ERK were purchased from Cell Signaling Technology (Danvers, MA, USA). An anti-actin antibody was purchased from Santa Cruz Biotechnology (Santa Cruz, CA, USA). Antibodies against Hsp90 and Hsp70 were purchased from Enzo Life Sciences, Inc. (Farmingdale, NY, USA). Antibodies against cleaved PARP and HIF-1α were purchased from BD Biosciences (San Jose, CA, USA). The Ni-NTA agarose was purchased from Invitrogen (Carlsbad, CA, USA). The first-strand cDNA synthesis kit was purchased from Dakara Korea Biomedical Inc. (Seoul, Republic of Korea). The EconoTaq DNA polymerase was purchased from Lucigen Corp. (Middleton, WI, USA). 3-(4,5-dimethylthiazol-2-yl)-2,5-diphenyltetrazolium bromide (MTT), propidium iodide (PI), avidin-agarose, crystal violet, and other chemicals, unless otherwise specified, were purchased from Sigma-Aldrich (St. Louis, MO, USA).

Cell culture

HT-22 and RPE cells were cultured in DMEM supplemented with 10% fetal bovine serum (FBS) and antibiotics. Other cancer cells were cultured in RPMI 1640 medium supplemented with 10% FBS and antibiotics. BEAS-2B and HBE cells were maintained in K-SFM (Invitrogen) supplemented with EGF and bovine pituitary extracts. HUVECs were cultured in endothelial cell basal medium [EBM-2 (Lonza Inc., Allendale, NJ, USA)] supplemented with EGM-2 SingleQuots (Lonza). HUVECs between passages 3 and 8 were used. Cells were incubated at 37°C with 5% CO_2 in a humidified atmosphere.

Drug-resistant cells that have acquired resistance to paclitaxel (H226B/R and H460/R) and an IGF-1R TKI linsitinib (H292/R) were generated by continuous exposure to increasing concentrations of corresponding anticancer drugs for more than 6 months. H226B/K-Ras cells were generated by retroviral transduction of mutant K-Ras.

MTT assay

Cells (1-2 x 10^3 cells/well in 96-well plates) were treated with increasing concentrations of SH-1242 for 3 or 5 d. Cells were treated with MTT and incubated for 2-4 h at 37°C. The formazan products were dissolved in DMSO, and the absorbance was measured at 570 nm. The data are presented as percentages of the control group.

Anchorage-dependent and anchorage-independent colony formation

For the anchorage-dependent colony formation assay, cells were seeded onto 6-well plates at a density of 300 cells/well and then treated with increasing concentrations of SH-1242 for 2 weeks. The colonies were fixed with 100% methanol, stained with 0.005% crystal violet solution at room temperature, and then washed with deionized water 3-5 times. The colonies were photographed and counted. For the anchorage-independent colony formation assay, the cells were mixed with sterile 1% agar solution (final concentration of 0.4%) and then poured onto 1% base agar in 24-well plates. SH-1242, diluted in complete medium, was added to the agar after the top agar solidified. The cells embedded in the top agar were incubated for 2 weeks at 37°C with 5% CO_2. After incubation, the colonies were stained with MTT solution and then photographed and counted.

Tube formation assay

H1299 cells were treated with SH-1242 or deguelin for 1 d and then further incubated under normoxic or hypoxic conditions for 4 h. After incubation, the drug-containing medium was discarded and fresh serum-free medium was added to cell and further incubated for 24 h. After incubation, the conditioned medium (CM) was collected. The tube formation assay was performed as previously described (1). Briefly, the HUVECs were diluted in complete medium and seeded onto CellBIND surface 96-well plates (Corning). The cells were treated with the CM. The morphological changes of the HUVECs were photographed and scored.

Western blot analysis

Unless otherwise indicated, the cells were treated with various concentrations of SH-1242 for 2 d and then further incubated under normoxic or hypoxic conditions for an additional 4 h. Cell lysates were obtained using RIPA lysis buffer as previously described (2). Equal amounts (20-30 μg) of cell lysates were resolved using 8-15% SDS-PAGE and then transferred onto a PVDF membrane. The membranes were blocked with blocking buffer [3% BSA in PBS containing 0.1% Tween-20 (PBS-T)] for 1 h at room temperature and then incubated with primary antibodies diluted in blocking buffer (1:1000) overnight at 4°C. The membranes were washed three times with PBS-T for 1 h at room temperature and then incubated with the corresponding secondary antibodies diluted in 3% skim milk in PBS-T (1:5000-1:1000) for 1-2 h at room temperature. The membranes were washed three times with PBS-T for 1 h and then visualized using an enhanced chemiluminescence (ECL) detection kit (Thermo Fisher Scientific, Waltham, MA, USA).

RT-PCR

Total RNA was prepared using TRIzol reagent (Invitrogen) according to the manufacturer's recommended procedure. RT-PCR was performed as previously described (2). The primer sequences used in the PCR assays are as follows: human IGF2 forward, 5'- TCG TGC TGC ATT GCT GCT TAC CG-3'; human IGF2 reverse, 5'- GCT CAC TTC CGA TTG CTG GCC AT-3'; human VEGF forward, 5'- TCT CCC AGA TCG GTG ACA GT-3'; human VEGF reverse, 5'- GGG CAG AGC TGA GTG TTA GC-3'; human β-actin forward, 5'- ACT ACC TCA TGA AGA TC-3'; human β-actin reverse, 5'- GAT CCA CAT CTG CTG GAA-3'. The PCR products were separated using 2% agarose gel electrophoresis and then visualized using a Gel Doc EZ System (Bio-Rad Laboratories, Hercules, CA, USA).

Animal studies

For xenograft experiments, H1299 and H292 cells (5 x 10^6 cells/mouse) were subcutaneously injected into the right flank of 6-week old NOD/SCID or nude mice. For patient-derived tumor xenograft (PDX) experiments, tumors that had been passed more than 3 times

in mice were minced into 2-mm^3 pieces and subcutaneously inoculated into NOD/SCID mice. After the tumor volume reached 50-150 mm^3, the mice were randomly grouped and treated with vehicle and compounds as described in Materials and Methods. Tumor growth was determined by measuring the short and long diameters of the tumor with a caliper, and body weight was measured twice per week to monitor toxicity. The tumor volume was calculated using the following formula: tumor volume (mm^3) = (short diameter)^2 × (long diameter) × 0.5.

To determine whether SH-1242 can inhibit K-Ras-driven spontaneous lung tumor formation, the K-Ras (G12D) transgenic mouse model [kindly provided by Dr. Guillermina Lozano (MD Anderson Cancer Center, Houston, TX, USA)] was used in experiments. To accelerate lung tumor formation, we backcrossed the K-ras transgenic mice in a C57BL6/129/sv background into the FVB/N background, which is known for its relatively high incidence of spontaneous lung tumors (3). Three-month-old mice were randomized into two groups (n=5) and treated with vehicle or SH-1242 for 8 weeks. Tumor growth was monitored using the IVIS-Spectrum microCT and Living Image (ver. 4.2) software (PerkinElmer, Alameda, CA, USA). To facilitate tumor monitoring, registered axial respiratory-gated CT image analysis and a fluorescence image analyses using an MMPSense 680 probe (PerkinElmer; 2 nmol/150 μl in PBS) were performed in mice treated with SH-1242 or vehicle at 5 months of age as previously described (4,5). The mice were euthanized, and tumor formation was evaluated and compared with that of the vehicle-treated control group. Microscopic evaluations of lung tissue were also performed to measure mean tumor number (N) and volume (V) in a blinded fashion after hematoxylin and eosin (H&E) staining. The tumor volume was calculated using the following formula: V (mm^3) = (long diameter x short diameter^2)/2, and the tumor load was calculated using the following formula: mean tumor number (N) x mean tumor volume (V) in a blind fashion. The number and size of tumors were calculated in five sections uniformly distributed throughout each lung.

Binding titration experiments using fluorescence measurements

To examine the binding properties of SH-1242 to Hsp90, fluorescence-based

equilibrium binding experiments were performed (6). A full-length protein, truncated N- and C-terminal domain of Hsp90 were each equilibrated with various concentrations of ligands before measuring fluorescence emission. All titration experiments were conducted at 20°C using a Jasco FP 6500 spectrofluorometer (Easton, MD, USA). Ligand stock solutions were titrated into a protein sample dissolved in phosphate buffer (pH 7.4) containing 137 mM NaCl, 2.7 mM KCl, 10 mM Na_2HPO_4 and 2 mM KH_2PO_4. The total volume of DMSO used to solubilize the ligand was less than 2% in all cases. The proteins were excited at 285 nm, and the decrease of fluorescence emission at 340 nm after ligand binding was measured as a function of ligand concentration. All titration data were fit to a hyperbolic binding equation to obtain K_d values.

Homology modeling of the open conformation hHsp90 homodimer

The ligands were prepared in the Mol2 format using the sketch modules embedded in Sybyl. Gasteiger-Hückel charges were assigned to all ligand atoms. Each ligand was energy-minimized using a standard Tripos force field with convergence to maximum derivatives of 0.001 kcal/(mol·Å). The prepared ligands were saved in a database for docking simulations.

We conducted homology modeling of full-length of human Hsp90 using the ORCHESTRAR module. It has been reported that the function of Hsp90 C-terminal inhibitors is associated with binding to the open form of the homodimer Hsp90 structure (7). We built up an open conformation of the human Hsp90 dimer based on the extended SAXS model of the *E. coli* Hsp90 homodimer, including the N-, middle and C-terminal domains (8). The template structure was retrieved from the Agard lab web site (http://www.msg.ucsf.edu/agard, PDB id: hsp90). The sequence identity of Hsp90 between *E. coli* and humans is 42.9%. First, an alignment file was defined using a complete partial model. Then, based on this alignment file, the structurally conserved regions (SCRs) were built automatically, and the structurally variable region was identified. SCRs, including loops, were optimized using the loop-search option. The side chains were modified using the set side chain option. To optimize the protein structure, a minimization of model was performed by assigning Kollman-all charges to all of the atoms in the protein and koconvergence to maximum derivatives of 0.05 kcal mol^{-1} $Å^{-1}$.

Molecular docking

Flexible docking of SH-1242 in Hsp90 was performed using the Tripos Sybyl-X 2.1 (Tripos Inc., St. Louis, MO, USA) molecular modeling package on a CentOS Linux 5.4 operating system. All the compounds in the database were docked into the active site of the Hsp90 homology model structure using the Surflex-Dock algorithm. The active site was defined by generating a protomol based on the ATP-binding pocket of the C-terminal domain (7). The protomol was built in the active site from the hydrogen-containing protein mol2 file using the default parameters (threshold factor of 0.5 Å and bloat of 0 Å). Docking was performed with the default parameters and a maximum of 20 conformation numbers. The binding affinity of each docking pose of the ligand was calculated from the Surflex-Dock score (-log K_d). Based on the docking score and visual inspection, the top-ranked docking model was selected.

References

1. Oh SH, Woo JK, Jin Q, Kang HJ, Jeong JW, Kim KW, et al. Identification of novel antiangiogenic anticancer activities of deguelin targeting hypoxia-inducible factor-1 alpha. International journal of cancer Journal international du cancer 2008;122(1):5-14.
2. Oh SH, Woo JK, Yazici YD, Myers JN, Kim WY, Jin Q, et al. Structural basis for depletion of heat shock protein 90 client proteins by deguelin. Journal of the National Cancer Institute 2007;99(12):949-61.
3. Mahler JF, Stokes W, Mann PC, Takaoka M, Maronpot RR. Spontaneous lesions in aging FVB/N mice. Toxicologic pathology 1996;24(6):710-6.
4. Lee HY, Oh SH, Woo JK, Kim WY, Van Pelt CS, Price RE, et al. Chemopreventive effects of deguelin, a novel Akt inhibitor, on tobacco-induced lung tumorigenesis. Journal of the National Cancer Institute 2005;97(22):1695-9.
5. Clapper ML, Hensley HH, Chang WC, Devarajan K, Nguyen MT, Cooper HS. Detection of colorectal adenomas using a bioactivatable probe specific for matrix metalloproteinase activity. Neoplasia 2011;13(8):685-91.
6. Takahashi M, Altschmied L, Hillen W. Kinetic and equilibrium characterization of the Tet repressor-tetracycline complex by fluorescence measurements. Evidence for divalent metal ion requirement and energy transfer. Journal of molecular biology 1986;187(3):341-8.
7. Sgobba M, Forestiero R, Degliesposti G, Rastelli G. Exploring the binding site of C-terminal hsp90 inhibitors. Journal of chemical information and modeling 2010;50(9):1522-8.
8. Krukenberg KA, Southworth DR, Street TO, Agard DA. pH-dependent conformational changes in bacterial Hsp90 reveal a Grp94-like conformation at pH 6 that is highly active in suppression of citrate synthase aggregation. Journal of molecular biology 2009;390(2):278-91.

Supplementary Table 1. The acquisition of drug resistance in several drug resistant cells (designated '/R') upon corresponding anticancer drug treatment

Cell line	Anticancer drug	IC_{50}	
		Parental	Resistant
H292/R	Linsitinib	8.7 μM	35.1 μM
H226B/R	Paclitaxel	7.6 nM	192.1 nM
H460/R	Paclitaxel	4.1 nM	205.8 nM
PC-9/GR	Gefitinib	0.8 μM	16 μM

Supplementary Table 2. Docking and scoring known Hsp90 inhibitors into the C-terminal ATP binding pocket of Hsp90

Ligands	Surflex-Dock score (-log K_d)	Hsp90 target domain
EGCG	6.24	C
SH-1242	6.01	C
KU135	5.89	C
Ganetespib	5.77	N
Novobiocin	5.6	C
Deguelin	5.35	C/N
ATP	4.69	C/N
17-AAG	3.87	N
Geldanamycin	0.64	N

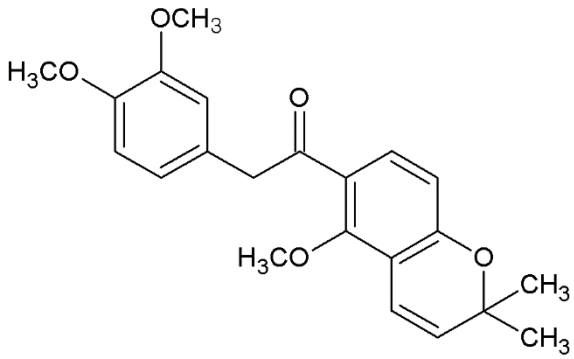

Supplementary Figure 1. Chemical structure of SH-1242.

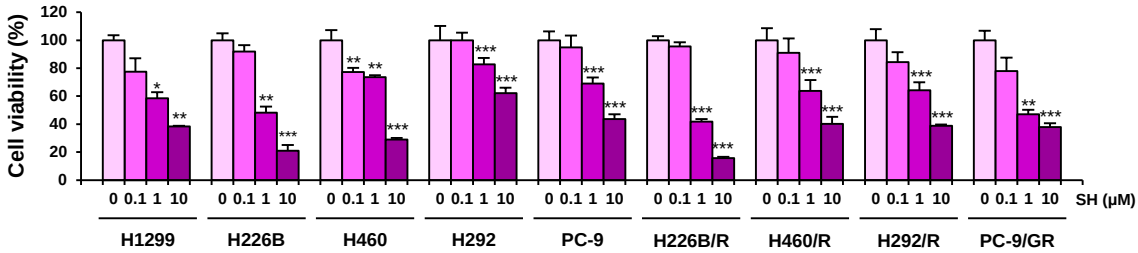

Supplementary Figure 2. Inhibitory effect of SH-1242 on the viability of a panel of human lung cancer cells with or without anticancer drug resistance.

The inhibitory effect of SH-1242 on cell viability was analyzed by the MTT assay. The bars represent the means ± SD; *: $P < 0.05$; **: $P < 0.01$; ***: $P < 0.001$, compared to vehicle-treated control.

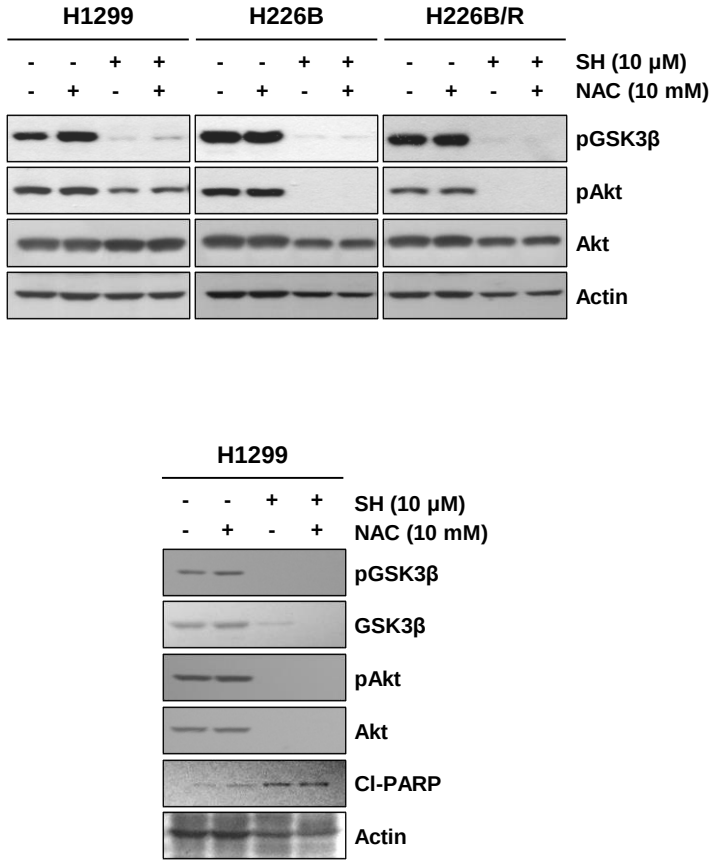

Supplementary Figure 3. Minimal involvement of ROS in the regulation of Akt phosphorylation and apoptosis induction mediated by SH-1242 treatment.

NSCLC cells were treated with SH-1242 (SH), alone or in combination with NAC for 24 h (*top*) or 48 h (*bottom*). Cell lysates were subjected to Western blot analysis.